American Mineralogist, Volume 74, pages 132–140, 1989

Major-cation substitution in phlogopite and evolution of carbonatite in the Potash Sulphur Springs complex, Garland County, Arkansas

RICHARD C. HEATHCOTE,* GEORGE R. MCCORMICK
Department of Geology, The University of Iowa, Iowa City, Iowa 52242, U.S.A.

ABSTRACT

The petrogenetic relationships among three carbonatite units in the Potash Sulphur Springs alkaline complex are interpreted using petrographically determined relative ages and mineral chemistry of phlogopite contained in the carbonatites. The oldest sovite (C_1) is interpreted to have magmatically differentiated to the youngest sovite (C_3). The intermediate-age alvikite (C_2) is interpreted to have formed by magma mixing of the C_1 sovite and residual ijolite magma. Composition of the hybrid C_2 alvikite was probably controlled in part by the degree of sovite magma evolution at the time of the mixing. The compositional trend from C_1 to C_3 sovite is Si and Mg enrichment and Al, Ti, and Fe depletion. Oxidation of Fe occurred concurrently with depletion of Al, causing the later phlogopite generations to incorporate Fe^{3+} in tetrahedral sites. The compositional evolution of carbonatitic phlogopites is generalized as the replacement of a hypothetical Ti analogue of siderophyllite [$A_2Fe^{2+}_3TiR^{3+}Si_4R^{3+}_4O_{22}$] by ferriphlogopite [$A_2Mg_6Si_6Fe^{3+}_2O_{22}$]. The phlogopite of C_2 alvikite differs from that in C_1 sovite by replacement of end-member phlogopite [$A_2Mg_6Si_6R^{3+}_2O_{22}$] with end-member annite [$A_2Fe^{2+}_6Si_6R^{3+}_2O_{22}$]. Similar compositions of phlogopite in alvikite, feldspathic fenite, and phlogopitized melteigitic and ijolitic rocks suggests that separate K-Al– and Mg-Fe–bearing fenitizations occurred when alvikite magma was present. Oscillatory zoning in phlogopites of C_2 and C_3 carbonatites suggest that quiescent conditions existed in alvikite and sovite magma chambers late in the evolution of these magmas.

INTRODUCTION

This investigation was designed to determine what major-element variations exist in micas in the carbonatite suite of the poorly exposed Potash Sulphur Springs intrusive complex, west-central Arkansas (Fig. 1), and to determine whether any observed variations can be used to reconstruct the petrogenesis of the carbonatite units in the absence of diagnostic field relations. Mica may provide a record of evolving magma composition because of the wide variety of cations that readily substitute in its various structural sites (Nockholds, 1947; Foster, 1960; Němec, 1972; Speer, 1984). Nockolds reported a range of Al_2O_3, MgO, and FeO proportions in micas from a variety of rock types and concluded that Al_2O_3 content, relative to MgO and FeO, is dependent on mineral paragenesis. Nockolds also concluded that the relative proportion of MgO and FeO is dependent on the degree of magma differentiation and is independent of paragenesis. Rimsaite (1969, p. 359) concluded that micas in the Oka carbonatite "represent the entire crystallization history" of that unit. Petrographic evidence from Oka reveals, according to Rimsaite, that discontinuous compositional shifts between zones in micas were caused either by resorption or by incipient crystallization of other minerals. This discontinuous variation is superimposed on gradual compositional variation caused by magmatic differentiation.

Major-cation variations in carbonatitic micas have been reported from Oka, Quebec (Rimsaite, 1969), Iron Hill, Colorado (Nash, 1972), occurrences in the Soviet Union and Uganda (Rass and Boronikhin, 1976), southern West Greenland (Secher and Larsen, 1980), Jacupiranga, Brazil (Gaspar and Wyllie, 1982), and central Arkansas (McCormick and Heathcote, 1987). Core-to-rim compositional variations in carbonatitic micas have been discussed by Nash (1972), Gittins et al. (1975), and Gaspar and Wyllie (1982). Eckerman (1948) and Vartiainen (1980) presented optical proof of carbonatitic phlogopite zonation and discussed the implications of this for magma differentiation. In this report, petrographic evidence for relative age is described for three carbonatites of the Potash Sulphur Springs complex, and the nature of major-cation substitution is interpreted for phlogopite that crystallized as these magmas evolved.

Magmatic phlogopite crystals selected for analysis possess sharp margins and euhedral to subhedral shapes; they are not altered. Phlogopite crystals that display anhedral shape and altered margins or cleavage traces are interpreted to be xenocrysts from elsewhere in the complex. The sources of the most common xenocrysts and xeno-

* Present address: 2825 Harmony Drive, Bakersfield, California 93306, U.S.A.

0003–004X/89/0102–0132$02.00

liths found in the Potash Sulphur Springs carbonatites are the ijolitic rocks and the fenites.

Methods of investigation

Mineral compositions were obtained from polished thin sections by energy-dispersive X-ray methods on ARL-EMX-SM microprobes at the University of Chicago and the University of Iowa. Microprobe standards for the major elements were natural minerals and synthetic silicate glasses; Kakanui hornblende was used as a working standard. Analytical precision estimated from repeated analyses of major oxides in Kakanui hornblende was ±6.2 relative percent or better at one standard deviation; the minimum detectable level for the elements of interest was 0.2 wt%. Reconnaissance analyses by wavelength-dispersive spectrometry indicated that F is present in all phlogopite populations of this study. Ba concentrations are below EDS detectability in all samples; thus interference of Ba *L*-series X-ray emission peaks with Ti *K*-series peaks is not significant in the analyses of this study. Analytical conditions were 15-μm spot size, 15-kV accelerating voltage at 100 nA, and 60-s counting time. Background and peak counts for the elements were determined with the procedures of Reed and Ware (1975); matrix corrections were made with the factors of Bence and Albee (1968).

Representative phlogopite and clinopyroxene analyses are given in Tables 1 and 2; all phlogopite analyses obtained were used in constructing Figures 2–6. Fe is reported as Fe^{2+}. Mineral formulas were not recalculated for Fe^{3+} although it is known to be present in some minerals. Vanadium ore occurs in the Potash Sulphur Springs complex, and V was detected in certain clinopyroxenes (Table 2), but standards for this element were not employed in the EDS routine so the significance of the recorded V value is unknown.

Geologic setting

The Potash Sulphur Springs complex is a subvolcanic structure, roughly circular in plan, with approximately 2.6-km^2 surface exposure (Fig. 1). Unpublished geophysical information indicates that the igneous body plunges steeply toward the Magnet Cove complex, 8 km to the east (D. R. Owens, pers. comm.). Syenites are the dominant outcropping rock types of the complex; small exposures exist of pyroxenite, melteigite, ijolite, malignite, nephelinite, phonolite, and carbonatite. Numerous lamprophyre dikes are also present (Hollingsworth, 1967; Howard, 1974), and sodic and potassic fenites are developed at the periphery of the complex. Natural exposure is limited owing to deep weathering and dense vegetation; however, large exposures were excavated on the east and north sides of the complex after Union Carbide Corpo-

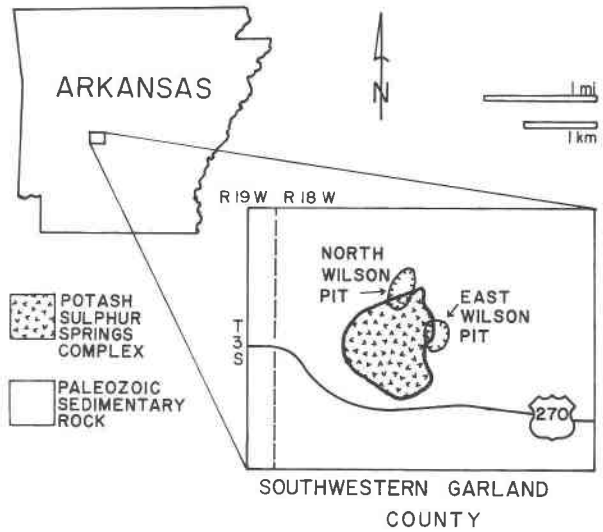

Fig. 1. Location of the Potash Sulphur Springs complex. Current exposure of the alkalic complex is within a folded and faulted sedimentary country-rock section that is dominated by massively bedded chert.

Table 1. Chemical composition of phlogopite (EDS microprobe data)

	Sovite (Ia)	Sovite (I)	Sovite (Ib)		Sovite (III)		Sovite pegmatite (IV)	Alvikite (II)			Melteigite (II)	Fenite (II)
	M439-2-1	M439-3-6	M307-1-8	M339-2-2	M488-2	M159-8-1	DG8-10-4	M173-10-1	BC-1-1	M15-5-4	BT-8-2	E73-1-4
SiO_2	34.59	36.11	39.97	38.44	41.44	44.66	35.24	37.09	38.95	40.36	38.35	41.62
TiO_2	2.68	3.88	0.95	1.35	0.97	0.36	3.13	2.84	2.26	1.17	1.83	2.03
Al_2O_3	15.46	16.40	13.61	12.58	11.37	9.32	11.83	12.02	11.23	11.14	11.96	11.74
FeO*	18.85	12.03	9.68	13.71	8.36	6.06	25.65	20.89	17.92	15.03	15.87	11.81
MnO	0.46	0	0.30	0.32	0.29	0	0	0.71	0.59	0.95	0.39	0.35
MgO	13.82	18.40	22.38	19.05	21.21	25.05	10.36	14.44	16.24	17.60	17.30	18.95
CaO	0.24	0.31	0	0	0.30	0.95	0.60	0	0.41	0.34	0.20	0
K_2O	9.91	10.28	9.93	9.53	10.38	11.19	10.01	10.50	10.29	9.99	10.35	10.21
Na_2O	0.46	0	0.32	0	0	0	0	0	0	0	0	0.36
Sum	96.47	97.41	97.14	94.98	94.32	97.59	96.82	98.49	97.89	96.58	96.25	97.07
Numbers of ions on the basis of 22 atoms of oxygen												
Si	5.27	5.25	5.72	5.74	6.07	6.26	5.54	5.59	5.80	5.98	5.75	6.01
Ti	0.31	0.42	0.10	0.15	0.11	0.04	0.37	0.32	0.25	0.13	0.21	0.22
Al	2.78	2.81	2.29	2.21	1.96	1.54	2.19	2.13	1.97	1.94	2.11	2.00
Fe*	2.40	1.46	1.16	1.71	1.02	0.71	3.37	2.63	2.23	1.86	1.99	1.43
Mn	0.06	0	0.04	0.04	0.04	0	0	0.09	0.07	0.12	0.05	0.04
Mg	3.14	3.98	4.77	4.24	4.63	5.23	2.43	3.24	3.60	3.89	3.86	4.08
Ca	0.04	0.05	0	0	0.05	0.14	0.10	0	0.06	0.05	0.03	0
K	1.93	1.90	1.81	1.81	1.94	2.00	2.01	2.02	1.95	1.89	1.98	1.88
Na	0.14	0	0.09	0	0	0	0	0	0	0	0	0.10

* Fe is reported as Fe^{2+}.

TABLE 2. Chemical composition of clinopyroxene (EDS microprobe data)

	Melteigite BT-1-3	Ijolite M185-cpx	Syenite KSS30a5	Fenite* DK-4-4	Alvikite BC-3-1	Alvikite** M15-4-4
SiO_2	48.21	51.45	52.60	53.32	51.61	43.70
TiO_2	2.20	0	0	1.06	0	4.30
Al_2O_3	5.32	1.37	0.95	0.47	0.34	7.64
FeO*	6.31	12.50	17.12	20.88	14.78	7.32
MnO	0	0.48	1.38	1.56	0.91	0
MgO	13.69	10.37	7.64	4.50	8.81	12.21
CaO	23.91	22.29	18.33	9.10	20.62	24.23
Na_2O	0.51	1.47	3.60	9.33	3.03	0
Sum	100.15	99.93	101.62	100.22	100.10	99.40
Numbers of ions on the basis of 6 atoms of oxygen						
Si	1.80	1.97	2.01	2.07	1.99	1.66
Ti	0.06	0	0	0.03	0	0.12
Al	0.23	0.06	0.04	0.02	0.01	0.34
Fe*	0.20	0.40	0.55	0.68	0.48	0.23
Mn	0	0.01	0.04	0.05	0.03	0
Mg	0.76	0.59	0.43	0.26	0.51	0.69
Ca	0.95	0.91	0.75	0.38	0.85	0.99
Na	0.04	0.11	0.27	0.70	0.23	0

* Contains ~0.92 wt% V_2O_3; Fe is reported as Fe^{2+}.
** Salite xenocryst in alvikite matrix.

ration commenced mining for vanadium in 1966 (Hollingsworth, 1967).

An Early Cretaceous (Albian) age of 100 ± 2 Ma was obtained for the Potash Sulphur Springs complex by U-Th-Pb dating of zircon (Zartman and Howard, 1985); Zartman et al. (1967) reported contemporaneous ages of 95 to 97 ± 5 Ma (K-Ar biotite) and 99 ± 8 Ma (Rb-Sr biotite) for syenitic rocks of the Magnet Cove complex. The ages of both complexes have been confirmed by fission-track dating of apatite and titanite (Eby, 1987). Both complexes were emplaced into Paleozoic sedimentary rocks that had been folded and faulted during the compressional, Pennsylvanian-Permian Ouachita orogeny. Very low grade (below greenschist facies) regional metamorphism in the Ouachita orogenic belt (Jackson, 1977; Guthrie et al., 1986) indicates current exposure is of a very shallow level in the subvolcanic structures.

Cretaceous alkaline igneous activity that included formation of the Potash Sulphur Springs complex spatially overlapped the Late Triassic tholeiitic province associated with Gulf of Mexico rifting (Moody, 1949; Brock and Heyl, 1961; Pilger, 1980; Edick and Byerly, 1981) and occurred adjacent to the Permian Wauboukigou alnoite province of southern Illinois and vicinity (Lewis and Mitchell, 1987). Cretaceous alkaline activity is closely associated with a belt of middle to Late Cretaceous uplift that extends from northwestern Louisiana to central Mississippi (Kidwell, 1951) including the Sabine and Monroe uplifts and the Jackson dome. The uplift belt crosses the axis of the Mississippi embayment, a regional downwarp also active in the Cretaceous, that developed over the late Precambrian Reelfoot aulacogen (Ervin and McGinnis, 1975). The Potash Sulphur Springs complex is located on the western margin of the Mississippi embayment, 160 km north of the uplift belt.

CARBONATITE PETROGRAPHY

Carbonatite samples were collected from a drillcore located near the center of the Potash Sulphur Springs complex (Heathcote, 1987) and from exposures in the northeast quadrant of the complex. Four carbonatite units were found to contain phlogopite. Rock names have been assigned following the guidelines of Streckeisen (1979); a single mineral prefix is used to distinguish the two sovites in this study.

Phlogopite sovite

Phlogopite sovite contains fine- to medium-grained apatite, magnetite, and phlogopite phenocrysts (1.0–>10.0 mm) in a mosaic-textured matrix of medium-grained (1.0–6.0 mm), inclusion-free calcite and minor dolomite; curved contacts between calcite crystals predominate. Rare xenocrysts of salite and melanite are present. Concentrations of magnetite, apatite, and phlogopite in some samples are suggestive of flow accumulations. Phlogopite is strongly pleochroic (X = pale yellow, Y = light green, Z = light green; $Z > Y > X$), and inclusion-free except for rare apatite.

Alvikite

Alvikite contains very fine grained phenocrysts (0.02–0.40 mm) of phlogopite, titanite, aegirine-augite, apatite, and nosean (nosean identified by optical properties and qualititative EDS analysis), with accessory magnetite and iron sulfide in a mosaic-textured matrix of fine-grained (0.3–1.5 mm), inclusion-rich calcite and minor dolomite. Apatite (0.02–0.07 mm diameter) has a distinctive oval outline in this carbonatite and occurs abundantly as inclusions in matrix carbonate. Planar contacts between adjacent carbonate crystals predominate, and flow banding is preserved in some specimens. Phlogopite phenocrysts commonly exhibit numerous concentric, optical zones and contain abundant inclusions of titanite, apatite, nosean, magnetite, iron sulfide, and melanite. Pleochroism of phlogopite is strong (X = pale yellow to orange, $Y = Z$ = green to red-brown).

Xenoliths of melteigite, ijolite, malignite, melanephelinite, and orthoclase fenite are common. Xenocrysts of green phlogopite, nepheline, perovskite, salitic to aegirine-augitic clinopyroxenes, melanite, orthoclase, and apatite are abundant in some specimens. Nepheline xenocrysts have been replaced by microcrystalline aggregates of cancrinite that have been subsequently mantled by nosean; perovskite is mantled by titanite. Melanite is typically replaced to some degree by calcite; salitic clinopyroxenes commonly exhibit margins altered to microcrystalline intergrowths of titanite, calcite, and arfvedsonite (arfvedsonite identified by qualitative EDS analysis). Green phlogopite xenocrysts (0.2–8.0 mm) from phlogopite sovite are invariably mantled by red-brown, magmatic phlogopite in the alvikite. Partial dissolution of xenocrystic phlogopite beneath alvikitic phlogopite mantles yields distinctive atoll-shaped aggregates of magmatic phlogopite in this unit. Atoll-phlogopite tends to

occur together with highly altered salite xenocrysts. Fragments of orthoclase and apatite appear unaltered in alvikite matrix.

Ferriphlogopite sovite

Ferriphlogopite sovite contains fine- to medium-grained phlogopite phenocrysts (0.1–3.0 mm), with accessory apatite, titanite, and pyrochlore, in a fine-grained (0.1–1.5 mm), mosaic-textured matrix of calcite and minor dolomite. Planar contacts between calcite crystals predominate in some samples; other samples exhibit extensive recrystallization with stylolites and strongly interpenetrative matrix calcite crystals. Dysanalyte (identified by optical character and qualitative EDS analysis), massive pyrrhotite, spherulitic clumps of zoned, limpid to inclusion-rich apatite, and an anastomosing network of unidentified green fibers are associated with stylolites. Xenoliths of alvikite and orthoclase fenite occur in this unit.

Ferriphlogopite commonly exhibits faintly visible oscillatory zoning and rarely contains apatite inclusions. Pleochroism ranges from weakly normal (X = pale yellow, $Y = Z$ = pale orange) to weakly reverse (X = orange, $Y = Z$ = pale orange). This mica is very similar in optical properties and composition to tetraferriphlogopite described by Puustinen (1973). Mössbauer spectra obtained from samples M159 (Table 1) and M213 (not shown) confirm the presence of tetrahedral Fe^{3+} in amounts of 36% ± 3% and 29% ± 3% of the Fe present in these two samples, respectively. The remaining Fe is octahedrally coordinated Fe^{2+} (M. D. Dyar, written comm., 1988).

Other carbonatites

Sovite pegmatite is the fourth mica-bearing carbonatite in the Potash Sulphur Springs complex. Biotite in this unit displays ragged crystal margins and is interpreted to be xenocrystic although it has not been found elsewhere in the complex. It is strongly pleochroic (X = red, $Y = Z$ = black). The sovite pegmatite, present in the East Wilson pit, cuts syenite and is cut by pyritiferous manganoan calcite veins. A fenite breccia with siderite matrix, present in the East Wilson pit, has been identified as ferrocarbonatite. This unit postdates orthoclase fenite, but is of uncertain age relative to other carbonatites.

Mineral chemistry of phlogopite

Compositional trends

Representative phlogopite and biotite analyses are presented in Table 1. Four separate types of phlogopite are determined by their optical characteristics and Al vs. Fe/(Fe + Mg) proportions (Fig. 2). The green phlogopite of phlogopite sovite is designated type I and is subdivided into subtypes I, Ia, and Ib on the basis of clusters evident in Figure 2. The red-brown to green phlogopite of alvikite is designated type II. Analyses from xenolith-poor alvikite samples plot within the dashed oval of Figure 2; micas with similar optical character occurring in silicate rocks scatter across the larger part of the type II field. Orange,

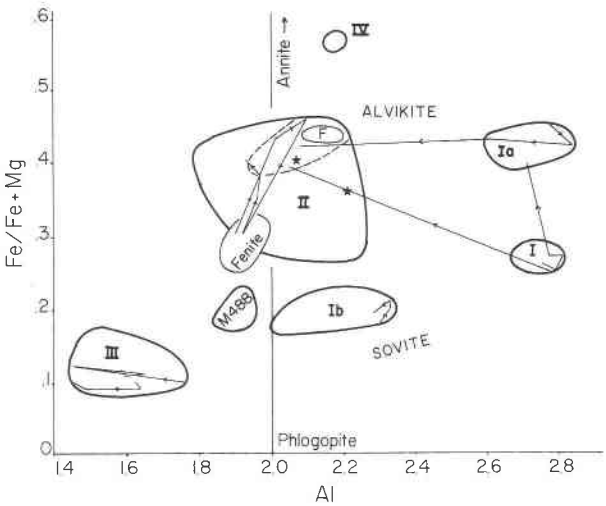

Fig. 2. Plot of Al (per 22 oxygen) vs. Fe/(Fe + Mg) for phlogopite; alvikite and sovite trends are designated as described in text. Enclosed fields correspond to phlogopite types described in text. Trend lines connect multiple analyses of single grains; arrows point rimward. Dashed oval in field II contains all analyses from xenolith-poor alvikites. Stars represent analyses from phlogopitized melteigite.

normal- to reverse-pleochroic phlogopite of ferriphlogopite sovite is designated type III. The field in Figure 2 labeled "M488" represents an aluminous ferriphlogopite population that is identified as type III by optical character. Biotite analyses from sovite pegmatite, designated type IV, cluster tightly at an Fe-enriched composition.

Relative ages of phlogopite compositional types are established by the consistent zoning sequences in individual crystals and by xenocrystic and crosscutting criteria. Examples of zoning and overgrowth sequences from individual grains are shown in Figures 2 and 4 to 6 by trend lines with arrows indicating the rimward direction. Phlogopite of subtype I occurs in sovite as unzoned crystals and in alvikite as cores of cryptically zoned crystals that bear rims of subtype Ia. Alvikite veins containing type II crystals cut sovite veins that contain subtype Ib crystals. Phlogopite subtypes Ib and I have not been found together, but occur in sovite samples that are similar to one another in grain size and mineral assemblage. Ferriphlogopite sovite contains xenoliths of alvikite that contain type II phlogopite. Based on these relationships, type III is determined to be the youngest of the phlogopites, subtype I is the oldest, and the intermediate-age type II is younger than subtypes Ia and Ib.

Inclusion and xenocryst relationships and phlogopite zoning stratigraphy are used, together with similarities of rock texture and mineral assemblage, to define the sovite trend (I → Ib → M488 → III) and the alvikite trend (Ia → II) shown in Figure 2. It is clear from the established age relationships that crystallization of type II phlogopite on the alvikite trend began later than subtype I crystal-

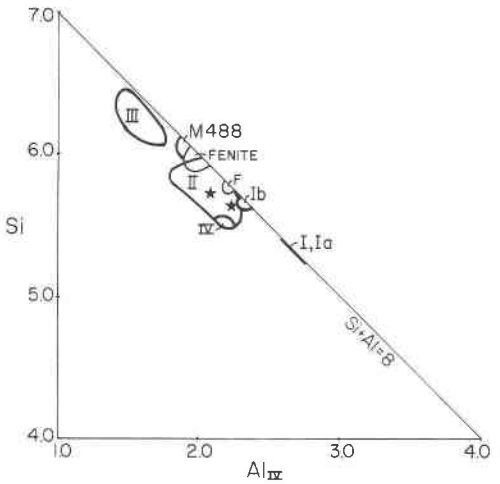

Fig. 3. Plot of tetrahedral Al vs. Si; symbols as in Fig. 2. Intrasite substitution line, Si + Al = 8, represents the dioctahedral-trioctahedral substitution. Subtype I phlogopite is the only population that consistently contains octahedrally coordinated Al. Tetrahedral Fe^{3+} is assumed for other types.

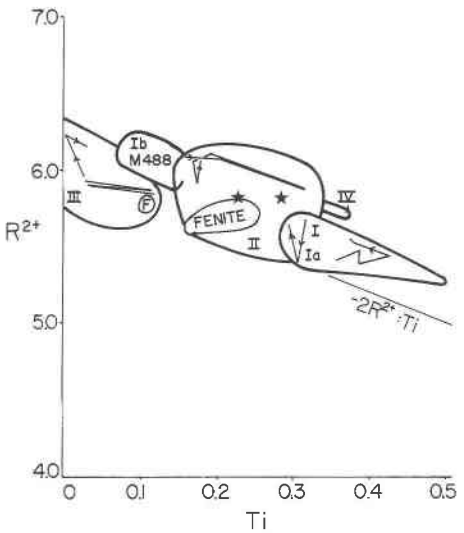

Fig. 4. Plot of Ti vs. R^{2+}; symbols as in Fig. 2. Intrasite substitution line, $-2R^{2+}$:Ti, represents the Ti-vacancy substitution. Subtype Ia phlogopite plots at the low-Ti end of the subtype I field; subtype Ib phlogopite and type III phlotopite of sample M488 are indistinguishable on this scattergram.

lization on the sovite trend, but ceased prior to crystallization of type III phlogopite on the sovite trend.

Cation substitutions

Phlogopite compositions provide a basis from which elemental changes in the evolving carbonatite magma can be determined. Specific cation substitutions are inferred from bivariate scattergrams where elongate data fields parallel permissible octahedral and tetrahedral substitution lines (Figs. 3–6). Because the EDS analyses in this study are limited to five major cations, the substitutions discussed below are the simplest among many choices (e.g., Hewitt and Abrecht, 1986) and are not claimed to be unique characterizations of phlogopite crystal chemistry in the Potash Sulphur Springs carbonatites. Uncertainties in A-site and anionic substitutions preclude a detailed mica-component exchange analysis. Intrasite substitutions (substitution restricted to either octahedral or tetrahedral sites) that fit the data are dioctahedral-trioctahedral ($^{[6]}R^{3+}{}^{[4]}R^{3+} = {}^{[6]}R^{2+}{}^{[4]}Si$; Fig. 3), annite-phlogopite ($Fe^{2+} = {}^{[6]}Mg$; Fig. 2), and Ti vacancy ($Ti = 2{}^{[6]}R^{2+}$; Forbes and Flower, 1974; Fig. 4). Alignments of data fields along intersite substitution trends (paired substitutions in octahedral and tetrahedral sites), corresponding to the given intrasite substitutions, are shown in Figures 5 and 6. Elongation of the type II and III fields perpendicular to the $Si:R^{2+}$ trend (Fig. 5) is an artifact caused by the assumption that total Fe is octahedrally coordinated Fe^{2+} when a portion is actually tetrahedrally coordinated Fe^{3+}. Tetrahedral Fe^{3+} is assumed, in the absence of Mössbauer analysis, for phlogopite types II, III, and some of subtype Ib because Si + Al sums are less than 8.00.

Alignments parallel to the trends $-2R^{2+}$:Ti (Fig. 4) and $2Si:R^{2+}$ (Fig. 5) suggest operation of the Ti-Tschermak substitution ($^{[6]}Ti2{}^{[4]}R^{3+} = {}^{[6]}R^{2+}2{}^{[4]}Si$, e.g., Czamanske and Wones, 1973; Robert, 1976), however, the $2Si:R^{2+}$ part of this substitution requires a much steeper slope for Mg vs. Si (ideally 1:2) than is evident for the broad 4Mg:Si alignment in Figure 6. No simple combination of Ti-Tschermak and other substitutions can produce the observed alignment. Simultaneous exchange of 2Mg for Ti, of Mg for Fe^{2+} and of Mg + Si for $^{[6]}R^{3+} + {}^{[4]}R^{3+}$ in the previously noted substitutions does yield the 4Mg:Si ratio.

A general characterization of the cation substitutions given above may be made in terms of ideal, anhydrous mica end-members. The depletion of Fe^{2+}, Ti, and Al, enrichment of Mg and Si, and Fe oxidation of the sovite trend correspond to replacement of a hypothetical Ti analogue of siderophyllite $[A_2({}^{[6]}Fe^{2+}_3TiR^{3+})(Si_4{}^{[4]}R^{3+}_4)O_{22}]$ by ferriphlogopite end-member $[A_2({}^{[6]}Mg_6)(Si_6{}^{[4]}Fe^{3+}_2)O_{22}$ (Annersten et al., 1971)]. Derivation of the alvikite trend from the sovite trend corresponds to replacement of phlogopite end-member $[A_2({}^{[6]}Mg_6)(Si_6{}^{[4]}R^{3+}_2)O_{22}]$ by annite end-member $[A_2({}^{[6]}Fe^{2+}_6)(Si_6{}^{[4]}R^{3+}_2)O_{22}]$. Substitutions along the alvikite trend are similar to those along the sovite trend, but Mg enrichment at the expense of Fe is less evident.

Discussion

Details of carbonatite magma genesis are obscure in the Potash Sulphur Springs complex. Gross relationships among fenites and the sovite, alvikite, and silicate magmas can be inferred from available inclusion relations.

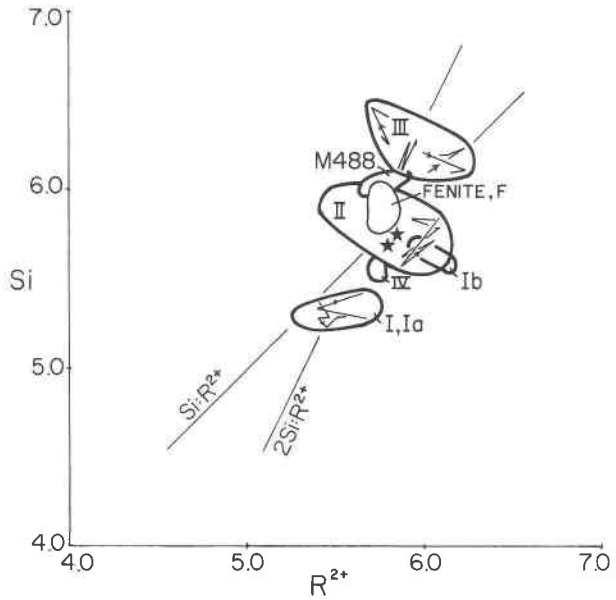

Fig. 5. Plot of R^{2+} vs. Si; symbols as in Fig. 2. Intersite substitution line, Si:R^{2+}, represents dioctahedral-trioctahedral substitution; 2Si:R^{2+} represents Ti-Tschermak substitution. Subtypes I and Ia are indistinguishable on this scattergram, as are the two fenite fields. Field II and III elongations along the −Si:R^{2+} trend are caused by assumption that all Fe is octahedrally coordinated Fe^{2+} when tetrahedrally coordinated Fe^{3+} is actually also present.

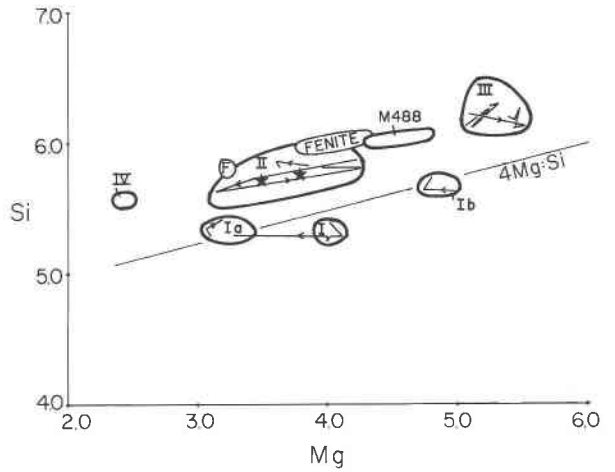

Fig. 6. Plot of Mg vs. Si; symbols as in Fig. 2. Intersite substitution ratio, 4Mg:Si, along which the data broadly trends, can result from combined dioctahedral-trioctahedral, annite-phlogopite, and Ti-vacancy substitutions acting in unison toward Mg enrichment.

Differentiation of the parental Potash Sulphur Springs silicate magma may reasonably be assumed to have produced a petrogenetic sequence such as that documented for other complexes (e.g., King, 1965; Sørensen, 1974; LeBas, 1977; Robins, 1980), wherein early pyroxenite or melteigite is succeeded by ijolite or malignite, with syenites forming latest. Clinopyroxenes crystallizing during differentiation of this sequence grade from salitic toward acmitic compositions (e.g., Nash, 1972). The presence of salite xenocrysts and the absence of aegirine-augite in phlogopite sovite of the Potash Sulphur Springs complex indicate that sovite formed later than salite-bearing pyroxenite and melteigite and possibly prior to the formation of aegerine-augite–bearing ijolite and malignite. Furthermore, subtype I phlogopite contains the highest proportion of Ti siderophyllite component in the complex, which indicates that it formed at higher temperature or pressure (e.g., Robert, 1976) than the other phlogopite types.

The presence in alvikite of abundant sovitic, type I phlogopite xenocrysts and unaltered, ijolitic, aegirine-augite xenocrysts indicates that alvikite is intimately linked with sovite and ijolite; salite xenocrysts from melteigite exhibit reacted margins in alvikite. Alvikite contains magmatic (euhedral) titanite, aegirine-augite, nosean, and melanite; it is mineralogically similar to ijolite. For these reasons, and the established relative ages of phlogopite types, alvikite is interpreted to have formed as a hybrid magma when ascending sovite magma encountered a pocket of residual ijolitic magma (Fig. 7). The abundance in alvikite of ijolitic xenoliths and xenocrysts is interpreted to indicate that the ijolite magma pocket was mostly crystalline at the time of the encounter with sovite magma, and only a residual, interstitial ijolitic liquid was present. An additional indication of the interpreted petrogenetic relationship is the similar cation ratios found between salitic clinopyroxene and type I phlogopite and between aegirine-augite and type II phlogopite. The parallel variations of Si, Al, Ti, Mg, Fe, and Fe oxidation evident between clinopyroxenes contained in melteigite and ijolite and between phlogopites contained in phlogopite sovite and alvikite also suggest the interpreted petrogenesis (Tables 1 and 2).

Subtype Ia phlogopite is found only in zoned xenocrysts in alvikite, indicating that it is not a crystallization product of sovite magma. It is suggested that subtype Ia represents a transient stage of Fe uptake by phlogopite that occurred between the initial encounter of sovite with the more Fe-rich ijolite and the subsequent formation of alvikite magma. After subtype Ia crystallized, the alvikite magma abruptly began to crystallize type II phlogopite, which involved an increase in available Si and depletion of Al over what had been available during crystallization of subtype Ia.

The petrogenetic relationship between fenitized rocks and carbonatites of the Potash Sulphur Springs complex remains obscure, but the following relationships have been found in this study. Some orthoclase fenite samples ("F," Figs. 2–6) contain type II phlogopite, whereas others ("Fenite," Figs. 2–6) contain phlogopite on an edge of the type II field, with tetrahedral Fe^{3+} similar to the type III

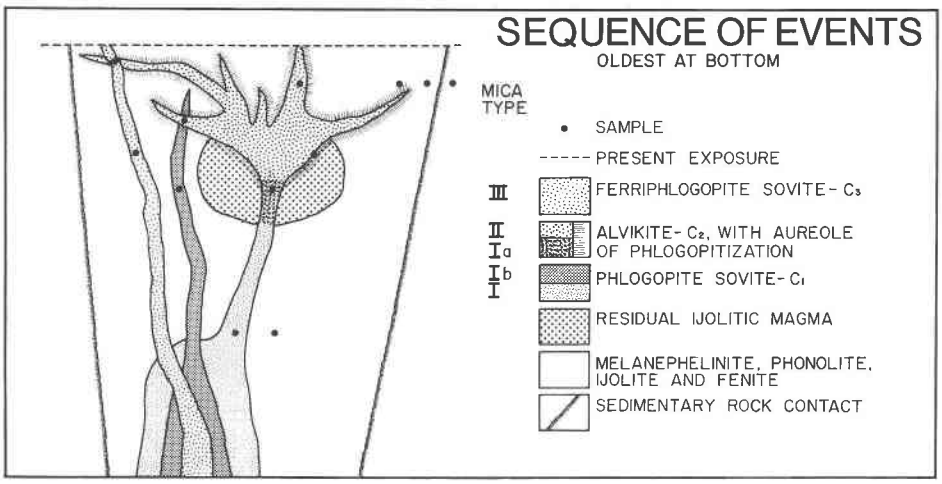

Fig. 7. Schematic representation of magmatic activity in the Potash Sulphur Springs complex between the time of phlogopite sovite (C_1) formation and later solidification of ferriphlogopite sovite (C_3). This period is interpreted to have preceded the formation of syenite. Relative ages of magmatic units are indicated by crosscutting. Dots noted as sample points represent sample coverage of the geologic units and crosscutting relationships discussed in text. Mica types are noted adjacent to the units in which they are found.

composition of sovite specimen M488 (Fig. 2). The presence of orthoclase fenite xenoliths (fenitized chert) in alvikite indicates that the alvikite magma formed after K-Al–bearing fenitization, but the presence of type II phlogopite in phlogopitized silicate rocks, and also in some samples of orthoclase fenite, suggests that a Mg-Fe–bearing fenitization event followed K-Al–bearing fenitization and coincided with the presence of alvikite magma. The drop in Al content between subtype Ia and type II phlogopite on the alvikite trend may relate to feldspathic (K-Al–bearing) fenitization of the chert country rock.

The presence of alvikite and fenite xenoliths in ferriphlogopite sovite indicates that evolution of sovite magma, from crystallization of subtype I to crystallization of type III phlogopite, bracketed the formation and solidification of alvikite magma. Oxidation of Fe in sovite to produce ferriphlogopite must have occurred during or after the suggested Mg-Fe metasomatism. The sovite magma apparently solidified prior to the formation of syenite and sovite pegmatite.

Oscillatory zoning in late-formed phlogopites of both alvikite and sovite suggests these magmas were not strongly stirred prior to solidification, but experienced instead a quiescent period that permitted expression of subtle crystal-liquid interface processes, similar to what has been proposed to produce oscillatory zoning in igneous plagioclases (e.g., Allègre et al., 1981). In earlier (hotter) magmatic stages, conditions for oscillatory zoning either did not occur or such zoning was obscured by ionic diffusion in the micas as suggested by Loomis (1983). Oscillatory zoning in alvikitic phlogopite involves exchange of Ti siderophyllite and ferriphlogopite components (Figs. 2 and 4). The zoning in ferriphlogopite sovite is more subdued than in alvikite and is dominated by exchange of Si and Al; Fe^{3+} evidently is not involved (Fig. 2). This difference in phlogopite oscillatory zoning between the two carbonatites may be due to the relative depletion of Fe and Al in late-stage sovite magma compared to alvikite magma.

A modification of the standard designation for carbonatites (LeBas, 1977, p. 268) is applied to units of the Potash Sulphur Springs complex on the basis of relative ages determined in this study: C_1 = phlogopite sovite (phlogopite subtypes I and Ib), C_2 = alvikite (type II), and C_3 = ferriphlogopite sovite (type III). In the standard designation, ferrocarbonatite is usually designated C_3. Later carbonatites are also present, but their place in the evolution of the complex is not clear.

Sovite magma (C_1) remained mineralogically simple, crystallizing phlogopite, magnetite, and apatite, until late in its history (C_3) when other minerals (e.g., pyrochlore) formed. The relative abundance of calcite and dolomite did not change appreciably during this evolution. Compositional evolution of sovite, as recorded in phlogopite, involved progressive Mg and Si enrichment and Fe, Ti, and Al depletion concurrent with Fe oxidation.

Alvikite magma (C_2) is interpreted to have formed when sovite magma (C_1) encountered residual ijolite magma. Alvikite magma then evolved rapidly to a relatively uniform composition richer in Si, Fe, and Ti (Ti as titanite) than sovite magma. The presence of magmatic nosean (with Na:K estimated as 7:1) in alvikite indicates that this magma also contained sulfate and was enriched in alkalies relative to sovite. This means that alkalies must have been contributed by the ijolite magma when alvikite magma formed.

The Fe depletion and Si and Mg enrichment of carbonatite determined in this study mirrors the cation movement in fenitization of metapelites by carbonatite that has been suggested by Mian and LeBas (1987), but

Al depletion evident in carbonatite of the Potash Sulphur Springs complex contrasts with the Al movement from wallrock toward carbonatite inferred by those authors.

The petrogenetic relationship between C_2 and C_3 carbonatites is interpreted to be purely accidental. The mixing event between silicate and C_1 carbonatite magmas could easily have occurred at a later stage, if at all, in the separate evolutions of the original magmas and then would have yielded different mineral assemblages and a different carbonatite suite.

Acknowledgments

We want to express our gratitude to Norman F. Williams, Director of the Arkansas Geological Commission, for the generous financial support furnished by the Commission for instrument and time charges for microprobe analyses. Sigma Xi and the Graduate College of the University of Iowa kindly furnished partial subsidy for drafting and photographic charges. We wish especially to thank Don R. Owens (Hot Springs, Arkansas) and Union Carbide Corporation for hospitality, help, and access to the Wilson Springs Vanadium Operation. J. V. Smith, as always, was most helpful in furnishing us with microprobe standards and allowing us time on the University of Chicago microprobe. The assistance and hospitality of Ian Steele and Rick Hervig during microprobe sessions at the University of Chicago are gratefully acknowledged. Reviews of an earlier draft of this paper by J. A. Speer and R. J. Arculus are much appreciated.

References cited

Allègre, C.J., Provost, A., and Jaupart, C. (1981) Oscillatory zoning: A pathological case of crystal growth. Nature, 294, 223–228.

Annersten, H., Devanarayanan, S., Haggstrom, L., and Wappling, R. (1971) Mössbauer study of synthetic ferriphlogopite $KMg_3FeSi_3O_{10}(OH)_2$. Physica Status Solidi (b), 45, K137 (not seen; extracted from Contributions to Mineralogy and Petrology, 77, 294, 1981).

Bence, A.E., and Albee, A.L. (1968) Empirical correction factors for the electron microanalysis of silicates and oxides. Journal of Geology, 76, 383–403.

Brock, M.R., and Heyl, A.V., Jr. (1961) Post-Cambrian igneous rocks of the central craton, western Appalachian mountains and Gulf Coastal plain of the United States. U.S. Geological Survey Professional Paper 424-D, D33–D35.

Czamanske, G.K., and Wones, D.R. (1973) Oxidation during magmatic differentiation, Finnmarka complex, Oslo area, Norway: Part 2. The mafic silicates. Journal of Petrology, 14, 349–380.

Eby, G.N. (1987) Fission-track geochronology of the Arkansas alkaline province. U.S. Geological Survey Open-File Report 87-0287.

Eckermann, H. von. (1948) The alkaline district of Alno Island. Sveriges Geologiska Undersökning, Ser. Ca, no. 36, 176 p.

Edick, M.J., and Byerly, G.R. (1981) Post-Paleozoic igneous activity in the southeastern United States. Geological Society of America Abstracts with Programs, 13, 236.

Ervin, C.P., and McGinnis, L.D. (1975) Reelfoot rift: Reactivated precursor to the Mississippi embayment. Geological Society of America Bulletin, 86, 1287–1295.

Forbes, W.C., and Flower, M.F.J. (1974) Phase relations of titan-phlogopite, $K_2Mg_4TiAl_2Si_6O_{20}(OH)_4$: A refractory phase in the upper mantle? Earth and Planetary Science Letters, 22, 60–66.

Foster, M.D. (1960) Interpretation of the composition of trioctahedral micas. U.S. Geological Survey Professional Paper 354-B.

Gaspar, J.C., and Wyllie, P.J. (1982) Barium phlogopite from the Jacupiranga carbonatite, Brazil. American Mineralogist, 67, 997–1000.

Gittins, J., Hewins, R.H., and Laurin, A.F. (1975) Kimberlite-carbonatite dikes of the Saguenay river valley, Quebec, Canada. In L.H. Ahrens, J.B. Dawson, A.R. Duncan, and A.J. Erlank, Eds., Physics and chemistry of the earth, 9, 137–148. Pergamon, New York.

Guthrie, J.M., Houseknecht, D.W., and Johns, W.D. (1986) Relationships among vitrinite reflectance, illite crystallinity, and organic geochemistry in Carboniferous strata, Ouachita Mountains, Oklahoma and Arkansas. American Association of Petroleum Geologists Bulletin, 70, 26–33.

Heathcote, R.C. (1987) Mica compositions and carbonatite petrogenesis in the Potash Sulphur Springs intrusive complex, Garland county, Arkansas. Ph.D. thesis, University of Iowa, Iowa City, Iowa.

Hewitt, D.A., and Abrecht, J. (1986) Limitations on the interpretation of biotite substitutions from chemical analyses of natural samples. American Mineralogist, 71, 1126–1128.

Hollingsworth, J.S. (1967) Geology of the Wilson Springs vanadium deposits, Garland County, Arkansas. Arkansas Geological Commission field-trip guidebook—Central Arkansas economic geology and petrology, 22–28.

Howard, J.M. (1974) Transition element geochemistry and petrography of the Potash Sulfur Springs intrusive complex, Garland County, Arkansas. M.S. thesis, University of Arkansas, Fayetteville, Arkansas.

Jackson, K.C. (1977) Analcite as a temperature indicator of Arkansas Ouachita deformation. Arkansas Geological Commission—Symposium on the geology of the Ouachita Mountains, vol. 2.

Kidwell, A.L. (1951) Mesozoic igneous activity in the northern Gulf Coastal plain. Transactions of the Gulf Coast Association of Geological Societies, 1, 182–199.

King, B.C. (1965) Petrogenesis of the alkaline igneous rock suites of the volcanic and intrusive centers of eastern Uganda. Journal of Petrology, 6, 67–100.

LeBas, M.J. (1977) Carbonatite-nephelinite volcanism. Wiley, New York.

Lewis, R.D., and Mitchell, R.H. (1987) Alnoite intrusion associated with Permian rifting in the New Madrid seismic rift complex. Geological Society of America Abstracts with Programs, 19, 745–746.

Loomis, T.P. (1983) Compositional zoning of crystals: A record of growth and reaction history. In S.K. Saxena, Ed., Kinetics and equilibrium in mineral reactions, p. 1–60. Springer-Verlag, New York.

McCormick, G.R., and Heathcote, R.C. (1987) Mineral chemistry and petrogenesis of carbonatite intrusions, Perry and Conway Counties, Arkansas. American Mineralogist, 72, 59–66.

Mian, I., and LeBas, M.J. (1987) The biotite-phlogopite series in fenites from the Loe Shilman carbonatite complex, NW Pakistan. Mineralogical Magazine, 51, 397–408.

Moody, C.L. (1949) Mesozoic igneous rocks of the northern Gulf Coastal plain. American Association of Petroleum Geologists Bulletin, 33, 1410–1428.

Nash, W.P. (1972) Mineralogy and petrology of the Iron Hill carbonatite complex, Colorado. Geological Society of America Bulletin, 83, 1361–1382.

Němec, D. (1972) Micas of the lamprophyres of the Bohemian massif. Neues Jahrbuch für Mineralogie Abhandlungen, 117, 196–216.

Nockolds, S.R. (1947) The relation between chemical composition and paragenesis in the biotite micas of igneous rocks. American Journal of Science, 245, 401–420.

Pilger, R.H., Jr., Ed. (1980) The origin of the Gulf of Mexico and the early opening of the central North Atlantic ocean. Proceedings of a symposium at Louisiana State University, School of Geoscience, Baton Rouge, Louisiana.

Puustinen, K. (1973) Tetraferriphlogopite from the Siilinjarvi carbonatite complex, Finland. Geological Society of Finland Bulletin, 45, 35–42.

Rass, I.T., and Boronikhin, V.A. (1976) Indicator ratios of petrogenetic elements in zones within coexisting silicate minerals in carbonatites. Geochemistry International, 13, 154–160.

Reed, S.J.B., and Ware, N.G. (1975) Quantitative electron microprobe analysis of silicates using energy dispersive X-ray spectrometry. Journal of Petrology, 16, 499–519.

Rimsaite, J. (1969) Evolution of zoned micas and associated silicates in the Oka carbonatite. Contributions to Mineralogy and Petrology, 23, 340–360.

Robins, B. (1980) The evolution of the Lillebukt alkaline complex, Stjernoy, Norway. Lithos, 13, 219–220.

Robert, J.-L. (1976) Titanium solubility in synthetic phlogopite solid solution. Chemical Geology, 17, 213–227.

Secher, K., and Larsen, L.M. (1980) Geology and mineralogy of the Sarfartoq carbonatite complex, southern West Greenland. Lithos, 13, 199–212.

Sørensen, H., Ed. (1974) The alkaline rocks. Wiley, New York.

Speer, J.A. (1984) Micas in igneous rocks. Mineralogical Society of America Reviews in Mineralogy, 13, 299–356.

Streckeisen, A. (1979) Classification and nomenclature of volcanic rocks, lamprophyres, carbonatites, and melilitic rocks: Recommendations and suggestions of the IUGS Subcommission on the Systematics of Igneous Rocks. Geology, 7, 331–335.

Vartiainen, H. (1980) The petrography, mineralogy, and petrochemistry of the Sokli carbonatite massif, northern Finland. Geological Society of Finland Bulletin, 313.

Zartman, R.E., and Howard, J.M. (1985) U-Th-Pb ages of large zircon crystals from the Potash Sulfur Springs igneous complex, Garland County, Arkansas. Geological Society of America Abstracts with Programs, 17, 198–199.

Zartman, R.E., Brock, M.R., Heyl, A.V., and Thomas, H.H. (1967) K-Ar and Rb-Sr ages of some alkaline intrusive rocks from central and eastern United States. American Journal of Science, 265, 848–870.

Manuscript received January 7, 1988
Manuscript accepted September 26, 1988